On the formation of a fast thermospheric zonal wind at the magnetic dip equator

T. Kondo,[1] A. D. Richmond,[2] H. Liu,[3] J. Lei,[4] and S. Watanabe[1]

Received 25 February 2011; revised 6 April 2011; accepted 6 April 2011; published 20 May 2011.

[1] Simulations with the NCAR Thermosphere - Ionosphere - Electrodynamics General Circulation Model (TIE-GCM) have been carried out to understand the cause of strong thermospheric zonal wind at the magnetic dip equator. The simulations show that the zonal winds blow strongly at the magnetic dip equator instead of at the geographic equator due to the latitude structure of ion drag. The fast winds at the dip equator are seen throughout the altitude between 280 km and 600 km, and the wind above 400 km is mainly accelerated via viscosity. A test simulation without viscosity verifies that the extension of the fast equatorial wind to heights above 400 km is maintained by viscous coupling with the winds at lower altitudes, in spite of there being an ion-drag maximum instead of relative minimum at the dip equator at high altitudes. Basically, viscosity is not so large compared to the pressure gradient and ion drag, but dynamics causes the pressure gradient and ion drag approximately to balance, and viscosity becomes important. The simulation results are consistent with the observations by the DE-2 and CHAMP satellites. Therefore we suggest that the zonal wind velocity in the low latitude region is controlled by ion drag and viscosity. **Citation:** Kondo, T., A. D. Richmond, H. Liu, J. Lei, and S. Watanabe (2011), On the formation of a fast thermospheric zonal wind at the magnetic dip equator, *Geophys. Res. Lett.*, *38*, L10101, doi:10.1029/2011GL047255.

1. Introduction

[2] The thermal dynamics of the earth's upper thermosphere is mainly controlled by solar EUV radiation in low-middle latitude regions. Neutral density increases due to rising temperature on the dayside and decreases due to declining temperature on the night side. The pressure gradient caused by the density difference drives horizontal winds from day to night. Ion drag, viscosity, and the coriolis force also play an important role on the wind. *Rishbeth* [1972] suggested that the ion drag is the major factor limiting the wind speed.

[3] Research has revealed that the thermospheric zonal wind blows most strongly at the dip equator instead of at the geographic equator [*Raghavarao et al.*, 1991; *Coley et al.*, 1994; *Liu et al.*, 2009; *Watanabe and Kondo*, 2011]. These studies investigated satellite data from DE-2 and CHAMP. Both satellites show the fastest zonal wind at the dip equator. The fast wind is observed during 08-05 local time (LT) when the equatorial ionization anomaly (EIA) is developed [*Liu et al.*, 2009]. Those authors suggested that ion drag is the main cause for shifting the wind from the geographic equator to the dip equator.

[4] On the other hand, DE-2 observations [see *Watanabe and Kondo*, 2011, Figure 3] showed that the zonal wind in the topside ionosphere (above ~500 km) is also strong above the dip equator, despite the fact that ion density, and therefore ion drag, tend to maximize over the dip equator at these high altitudes. To understand the generation mechanism of fast neutral wind in the low latitude region, we carried out numerical simulations with the NCAR Thermosphere - Ionosphere - Electrodynamics General Circulation Model (TIE-GCM) model. The calculated winds are also compared with observations obtained by the DE-2 and CHAMP satellites.

2. TIE-GCM Model and Simulation Conditions

[5] The NCAR TIEGCM is a time-dependent, three-dimensional model of the thermosphere/ionosphere. It solves the equations of the fully coupled thermosphere and ionosphere self-consistently [*Dickinson et al.*, 1981; *Roble et al.*, 1988; *Richmond et al.*, 1992]. The horizontal resolution is 5 degree × 5 degree in geographic longitude and latitude, and the vertical resolution is 1/2 scale height. The lower boundary is approximately 97 km and the upper boundary is approximately 400–700 km, depending on solar activity. Migrating diurnal and semidiurnal tides from *Hagan and Forbes* [2002, 2003] are imposed at the lower boundary. In this study all simulations are run under constant geophysical conditions for March equinox (day number 80), high solar activity (F10.7 of 174.1) and mild magnetic activity (Kp of 2), and results are analyzed after a diurnally reproducible state has been attained, about ten days after the start of a simulation. The momentum equation for the thermospheric gas takes into account the pressure gradient, ion drag, viscous, and coriolis forces, along with momentum advection. Horizontal viscosity is ignored in this model. Since the main forces on the upper-thermospheric zonal winds are the pressure gradient, ion drag and viscosity, we simulated for three conditions to examine the dynamics of the wind: (1) default case; (2) no ion drag force on the zonal wind; and (3) no viscous force. Case (2) sets $\lambda_{xx}\,(U_i - U_n) + \lambda_{xy}\,(V_i - V_n) = 0$, where λ_{xx} and λ_{xy} are components of the ion-drag tensor, U_i and V_i are the zonal and meridional ion drift velocity (in the x and y directions, respectively), and U_n and V_n are the zonal and meridional wind velocity. (Since meridional ion drag at low latitudes

[1]Department of Earth and Planetary Science, Hokkaido University, Sapporo, Japan.
[2]High Altitude Observatory, National Center for Atmospheric Research, Boulder, Colorado, USA.
[3]Research Institute for Sustainable Humanosphere, Kyoto University, Uji, Japan.
[4]Department of Aerospace Engineering Sciences, University of Colorado at Boulder, Boulder, Colorado, USA.

0094-8276/11/2011GL047255

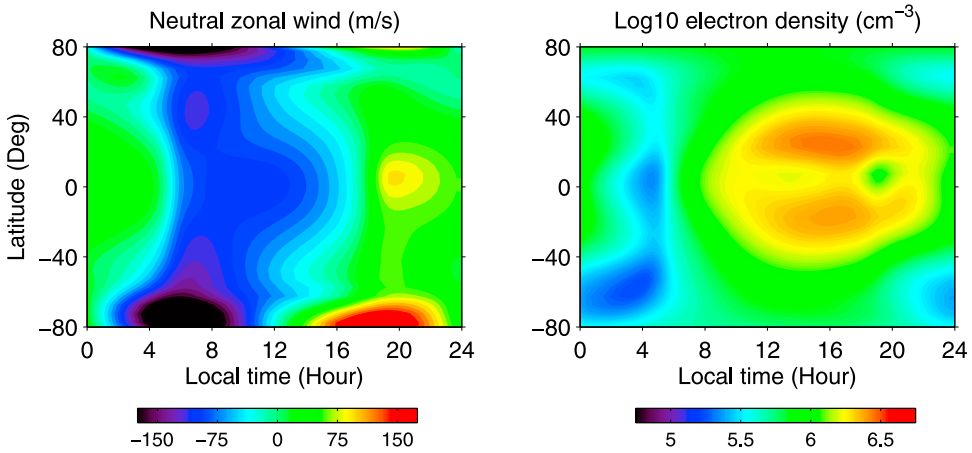

Figure 1. Latitude versus local time distributions of (left) the thermospheric zonal winds (positive eastward) and (right) the electron density about 400 km calculated by the TIEGCM, averaged over all longitudes at each local time.

tends to be much smaller than zonal ion drag, it was left unmodified.) Case (3) sets the viscosity coefficient to zero.

3. Results

[6] The thermospheric zonal wind and electron density distributions calculated by TIEGCM simulation in the frame of geographic latitude and local time, averaged over all longitudes at each local time, are presented in Figure 1. Roughly, the zonal wind velocity is westward during the day and eastward during the night. The eastward wind is strongest at about 20 LT at low latitude. The electron density forms an equatorial ionization anomaly (EIA) structure during 10-01 LT. The EIA structure is prominent during 18-22 LT due to the prereversal enhancement of the vertical drift [*Farley et al.*, 1986]. The electron density forms a large trough between ±10° latitude and the crest-trough-ratio (CTR) is largest in the afternoon and evening.

[7] Figure 2 is the latitude-longitude distribution of zonal wind at an altitude of about 400 km at 14 LT (Figure 2, left) and 20 LT (Figure 2, right). These are times when the EIA structure is well developed in the TIEGCM. Figures 2 (top) and 2 (bottom) show the zonal winds for the default model run (Case 1) and control run without ion drag (Case 2), respectively. In Figure 2 (top), the zonal wind blows strongly on the magnetic dip equator, where it is about −80 m/s (westward) at 14 LT and is about 100 m/s eastward at 20 LT. The fast flow at 20 LT is limited at a narrow latitudinal band which is aligned with the dip equator. This region corresponds to that of the electron density trough (see Figure 1). In Figure 2 (bottom), the velocity enhancements at the dip equator disappear and the zonal wind forms a maximum or minimum at the geographic equator. Therefore, we conclude that the zonal wind blows strongly at the magnetic dip equator due to the latitude structure of the ion drag force.

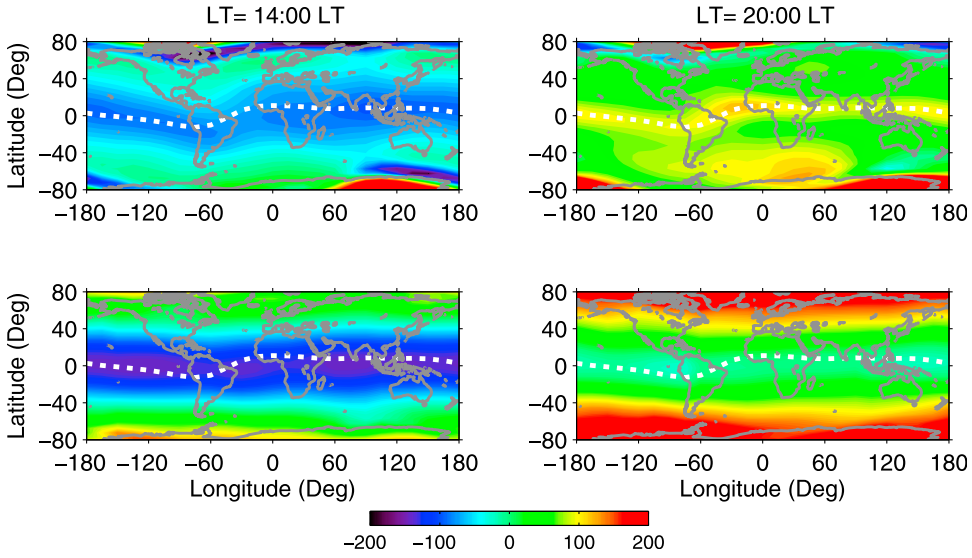

Figure 2. Thermospheric zonal wind distribution at (left) 14 LT and (right) 20 LT at about 400 km. (top) The default model run (Case 1) and (bottom) without ion drag (Case 2). The white dashed line is the dip equator. Positive wind values are eastward.

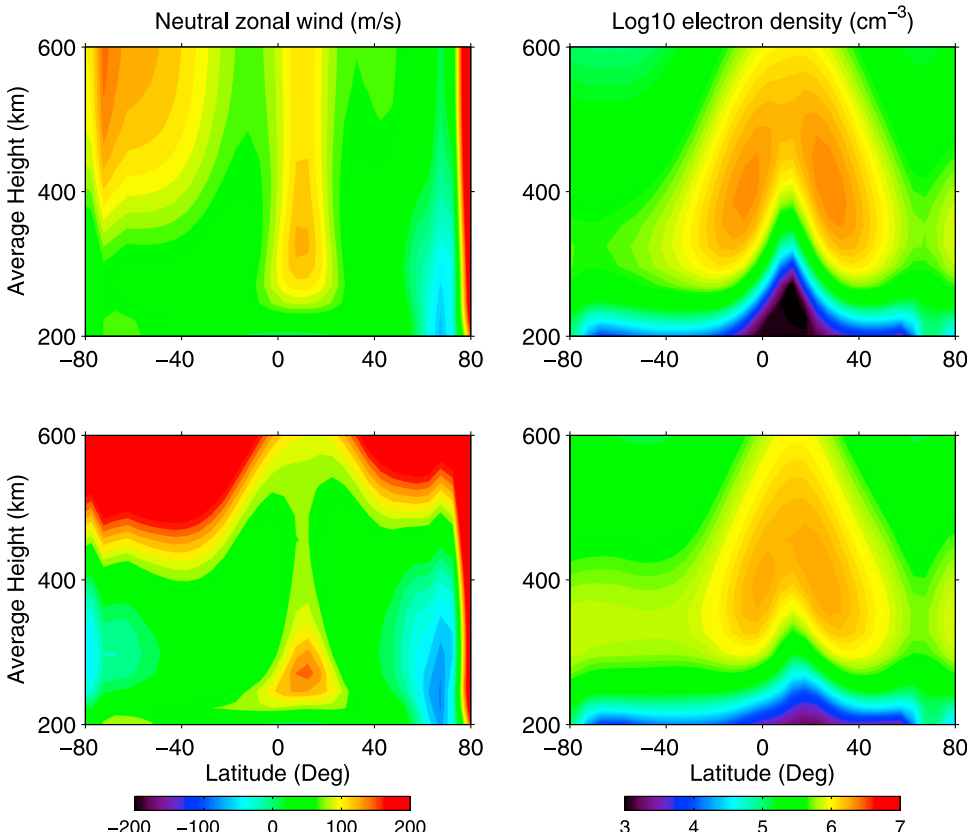

Figure 3. (left) The eastward zonal wind and (right) electron density altitude-latitude profiles at 20 LT and −15°E longitude. (top) Default conditions (Case 1) and (bottom) the no-viscosity condition (Case 3). The magnetic dip equator is at about 10°N geographic latitude.

[8] Figure 3 shows altitude-latitude distributions of the zonal wind (Figure 3, left) and the electron density (Figure 3, right) at −15°E longitude at 20 LT. Figures 3 (top) and 3 (bottom) show the default model run (Case 1) and no-viscosity run (Case 3), respectively. The zonal winds for the default run blow strongly eastward at the dip equator above about 250 km altitude, with maximum velocities in excess of 100 m/s between 300 km and 400 km. The CTR of the EIA electron density is largest between 300 km and 400 km, where the crest density is up to 10 times larger than the trough density. The EIA trough corresponds to a region of maximum zonal wind velocity. Above 450 km altitude, the zonal wind is still strong at the dip equator, even though the EIA trough disappears, and the electron density maximizes at the dip equator. Obviously, the zonal wind maximum above 450 km at the dip equator cannot be explained by the latitude structure of ion drag at those altitudes, as is the case below 400 km. The explanation lies rather in viscous coupling of the high-altitude winds with the winds below 400 km, where the atmosphere is denser.

[9] For Case (3), without viscosity (Figure 3, bottom), the zonal winds also blow strongly at the dip equator at an altitude of about 300 km, and the wind maximum corresponds to the electron density minimum. The notable feature is that the zonal winds above 400 km become weaker than for the default case, and the relative wind maximum at the dip equator disappears altogether above 550 km. Compared to the wind maximum at altitudes of 200–300 km, the zonal wind is about 100 m/s weaker above 350 km. Moreover, compared to the wind for the default run the zonal wind above 300 km is clearly weaker for the no-viscosity run. These features clearly show the effect of viscosity on the wind.

[10] Figure 4 shows the magnitude of the three major forces (pressure gradient, ion drag, and viscosity) and their sum at about 400 km altitude on the dip equator. Basically, the pressure-gradient and ion-drag forces are in approximate balance, so the zonal wind is westward when the pressure gradient is negative and eastward when it is positive. During

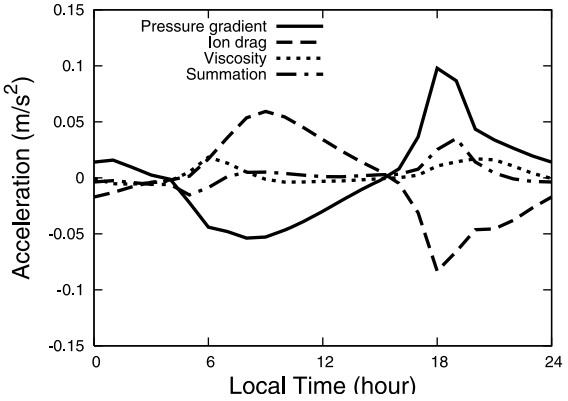

Figure 4. The diurnal variations of the three major terms in the zonal momentum equation and their sum at 400 km. Positive values are for eastward acceleration.

16–20 LT, the pressure gradient and ion drag terms change rapidly. These times are around sunset, where the atmospheric density starts to decrease. The viscosity term is weaker than the others. It is almost zero but is positive during 5–7 LT and 18–20 LT. The sum of all three terms is almost zero, but is negative during 4–7 LT when the wind is accelerating westward, and is positive during 17–20 LT when the wind is accelerating eastward.

[11] Although kinematic viscosity is expected to increase in importance with increasing altitude as the inverse of the air density, its relative contribution to the zonal acceleration at heights above 400 km (not shown) is found to be roughly comparable to its relative contribution at 400 km. Dynamically, all three forces (pressure gradient, ion drag, and viscosity) can react to the other forces in complex ways. Even when the viscous force is relatively small, it can nonetheless have an important influence on the dynamics.

4. Discussion and Summary

[12] Previous works revealed that thermospheric zonal winds blow strongly at the dip equator using DE-2 and CHAMP satellite data. Our results show the detailed properties of these winds for the first time using TIEGCM simulations.

[13] The zonal winds for the default run blow strongly at the dip equator, but blow strongly at the geographic equator when the ion drag is set to zero. This clearly indicates that the maximization of the zonal wind at the dip equator is due to the EIA structure of the ion drag force. The zonal wind measured by satellites also showed the fast zonal winds at the dip equator during local times of fully developed EIA [*Liu et al.*, 2009]. Our results are consistent with observation and strongly confirm that the latitude structure of the zonal wind is controlled by the plasma via ion drag.

[14] Other simulations also showed the fast zonal wind at the dip equator. *Anderson and Roble* [1974] examined the effect of vertical E × B drift on the thermospheric zonal wind at low latitudes using a thermospheric dynamics model. They showed that the fast zonal wind forms at the dip equator only when taking into account the postsunset upward E × B drift, which produces the EIA. Therefore, their and our results are consistent, which strongly confirms that the zonal winds blow strongly at the dip equator due to the EIA structure of ion drag.

[15] At the altitude of 300–400 km along the dip equator, the zonal winds form a latitudinal maximum and the electron density forms a latitudinal minimum. This feature was also shown by *Raghavarao et al.* [1991]. However, at middle latitudes, *Raghavarao et al.* [1991] showed that the minimum zonal velocity is found at about ±25° geomagnetic latitude at ~19 LT, while our results (see Figure 2 or 3) do not reproduce this feature. The reason for this is not clear yet.

[16] The EIA structure is seen at altitudes of about 250–450 km in Figure 3. But the zonal winds for the default case are still strong at the dip equator even at higher altitudes where the electron density no longer has a relative minimum, but rather maximizes at the dip equator. This velocity enhancement of zonal wind is also given by *Watanabe and Kondo* [2011] using DE-2 satellite data. They showed that the zonal wind blows strongly at the dip equator in the topside ionosphere during 18–24 LT. During that time in the region of the EIA, the crest of the zonal wind corresponds to the trough of electron density. From inspection of Figure 2, we determined that the thermospheric zonal wind blows along the dip equator due to the EIA structure of the ion drag. In the topside ionosphere, the zonal wind blows strongly at the dip equator due to another factor. The zonal wind at the dip equator at lower altitudes pulls that at upper altitudes via viscosity. Figure 3 (bottom) shows the zonal wind without viscosity. Here, the velocity enhancement of the zonal wind above the EIA is not seen, though it is seen in the default run. Furthermore, the zonal wind becomes weaker above the EIA region (>450 km) compared to that in the EIA region (<450 km). Of course changing viscosity in the momentum equation will also cause the other terms to change, as pressure gradients and ion drag adjust to the altered conditions. Therefore, Figure 3 does not show the effect of viscosity alone. However, changes in other effects like the ion drag coefficient are small, and viscosity is effective in affecting the wind, since the electron density does not change much compared to that in Figure 3 (top). Therefore, we suggest the zonal wind in the topside ionosphere above the EIA region is strongly affected by viscosity. Viscosity is not so large compared to the pressure gradient and ion drag, but dynamics causes the pressure gradient and ion drag approximately to balance, and viscosity becomes important. This approximate balance is also given by *Maruyama et al.* [2003], which uses a different numerical model of the thermosphere and ionosphere.

[17] In summary, we reveal two features of the equatorial thermospheric zonal wind. The first is that the zonal wind is strong at the dip equator instead of the geographic equator due to the larger ion drag at the crests of the EIA either side of the dip equator. The second is that the extension of the fast equatorial wind to heights above 400 km is maintained by viscous coupling with the winds at lower altitudes, in spite of there being an ion-drag maximum instead of relative minimum at the dip equator at high altitudes.

[18] **Acknowledgments.** This work was supported in part by NASA grants NNX09AN57G and NNX10AQ52G. The National Center for Atmospheric Research is sponsored by the National Science Foundation.

[19] The Editor thanks Philip Erickson and an anonymous reviewer for their assistance in evaluating this paper.

References

Anderson, D. N., and R. G. Roble (1974), The effect of vertical E × B ionospheric drifts on F region neutral winds in the low-latitude thermosphere, *J. Geophys. Res.*, *79*, 5231–5236, doi:10.1029/JA079i034p05231.

Coley, W. R., R. A. Heelis, and N. W. Spencer (1994), Comparison of low-latitude ion and neutral zonal drift using DE-2 data, *J. Geophys. Res.*, *99*, 341–348, doi:10.1029/93JA02205.

Dickinson, R. E., E. C. Ridley, and R. G. Roble (1981), A three-dimensional general circulation model of the thermosphere, *J. Geophys. Res.*, *86*, 1499–1512, doi:10.1029/JA086iA03p01499.

Farley, D. T., E. Bonelli, B. G. Fejer, and M. F. Larsen (1986), The prereversal enhancement of the zonal electric field in the equatorial ionosphere, *J. Geophys. Res.*, *91*, 13,723–13,728, doi:10.1029/JA091iA12p13723.

Hagan, M. E., and J. M. Forbes (2002), Migrating and nonmigrating diurnal tides in the middle and upper atmosphere excited by tropospheric latent heat release, *J. Geophys. Res.*, *107*(D24), 4754, doi:10.1029/2001JD001236.

Hagan, M. E., and J. M. Forbes (2003), Migrating and nonmigrating semidiurnal tides in the upper atmosphere excited by tropospheric latent heat release, *J. Geophys. Res.*, *108*(A2), 1062, doi:10.1029/2002JA009466.

Liu, H., S. Watanabe, and T. Kondo (2009), Fast thermospheric wind jet at the Earth's dip equator, *Geophys. Res. Lett.*, *36*, L08103, doi:10.1029/2009GL037377.

Maruyama, N., S. Watanabe, and T. J. Fuller-Rowell (2003), Dynamic and energetic coupling in the equatorial ionosphere and thermosphere, *J. Geophys. Res.*, *108*(A11), 1396, doi:10.1029/2002JA009599.

Raghavarao, R., L. E. Wharton, N. W. Spencer, H. G. Mayr, and L. H. Brace (1991), An equatorial temperature and wind anomaly (ETWA), *Geophys. Res. Lett.*, *18*, 1193–1196, doi:10.1029/91GL01561.

Richmond, A. D., E. C. Ridley, and R. G. Roble (1992), A thermosphere/ionosphere general circulation model with coupled electrodynamics, *Geophys. Res. Lett.*, *19*, 601–604, doi:10.1029/92GL00401.

Rishbeth, H. (1972), Thermospheric winds and the F-region: A review, *J. Atmos. Terr. Phys.*, *34*, 1–47, doi:10.1016/0021-9169(72)90003-7.

Roble, R. G., E. C. Ridley, A. D. Richmond, and R. E. Dickinson (1988), A coupled thermosphere/ionosphere general circulation model, *Geophys. Res. Lett.*, *15*, 1325–1328, doi:10.1029/GL015i012p01325.

Watanabe, S., and T. Kondo (2011), Ionosphere-thermosphere coupling in the low latitude region, in *Aeronomy of the Earth's Atmosphere and Ionosphere*, Springer, Berlin, in press.

T. Kondo and S. Watanabe, Department of Earth and Planetary Science, Hokkaido University, Sapporo, Hokkaido 060-0810, Japan. (kondou@ep.sci.hokudai.ac.jp)

J. Lei, Department of Aerospace Engineering Sciences, University of Colorado at Boulder, Boulder, CO 80309, USA.

H. Liu, Research Institute for Sustainable Humanosphere, Kyoto University, Gokasho, Uji, Kyoto 611-0011, Japan.

A. D. Richmond, High Altitude Observatory, National Center for Atmospheric Research, PO Box 3000, Boulder, CO 80307-3000, USA.